Proceedings of the 9th World Congress on Momentum, Heat and Mass Transfer (MHMT 2024)
London, United Kingdom – April 11 – 13, 2024
Paper No. ICMFHT 130
DOI: 10.11159/icmfht24.130

Experimental Investigation of Boiling Characteristics of High Volatile Fluids under Varying Heat Flux Levels

Alok Kumar[1], Mohammad Autif Shahdhaar[2], Atul Srivastava[1]
[1]Department of Mechanical Engineering, IIT Bombay, Powai-40076, India
alokra956@gmail.com; autifshahdhaar@gmail.com; atulsr@iitb.ac.in
[2]Center for Research in Nano Technology and Science, IIT Bombay, Powai-400076, India

Abstract **-** In recent years, there have been significant advances in the field of supercomputers and data centers, resulting in the generation of high heat flux levels. To effectively cool such high heat flux equipment, boiling immersion cooling has emerged as a promising solution. In the quest to enhance the heat transfer performance of nucleate boiling through passive means, this research focuses on exploring the boiling behavior of one of the high volatile fluids, namely dichloromethane (DCM). To investigate the nucleate boiling phenomenon of DCM, pool boiling experiments were conducted within a closed vessel at atmospheric pressure. Three distinct levels of heat flux were applied (58, 76, and 95 kW/m^2) to observe its impact on bubble dynamics. The experimental setup employed high-speed rainbow schlieren deflectometry to simultaneously map the dynamics of vapor bubbles while varying the heat flux levels. The results obtained from the experiments demonstrated a strong correlation between heat flux and various bubble characteristics. Specifically, the bubble mechanism, including bubble departure frequency, bubble diameter, waiting time, and forces acting on bubble, exhibited notable changes in response to variations in heat flux levels. By studying the bubble dynamics, it was observed that as the heat flux increased, the frequency at which bubbles departed from the heated surface decreased. Additionally, the bubble diameter was found to increase at higher heat flux levels. Furthermore, the waiting time, representing the duration between bubble departure and the subsequent bubble formation, as well as the various forces acting on bubble were also seen to be strongly influenced by the applied heat flux.

Keywords**:** Pool Boiling, High volatile fluid, Vapor bubble dynamics

1. Introduction

In recent years, the development of electronic technology has led to an increase in the heat generation density, particularly from semiconductor devices. Traditional cooling methods using air or single-phase liquid have limitations in managing the operating temperature of electronic devices, especially those with high heat density. This has prompted the exploration of alternative cooling techniques, such as liquid cooling utilizing nucleate boiling heat transfer, which offers advantages over conventional methods. The critical heat flux (CHF) plays a crucial role in determining the efficiency and safety of cooling systems. Systems often operate below the CHF limit to maintain safety margins, despite sacrificing efficiency. Understanding the mechanisms involved in heat transfer is essential for improving cooling performance. With the growing demand for effective heat dissipation in high heat flux devices, two-phase heat transfer, particularly pool boiling heat transfer, has garnered significant attention and proven to be reliable and efficient in various engineering fields, including high-performance electronics and nuclear reactors. Moreover, as electronic systems become smaller and heat exchangers more compact, conventional single-phase forced convection cooling methods are no longer sufficient. Immersion two-phase cooling with a highly volatile fluid has emerged as a viable solution, finding applications in spacecraft, computer chips, data centers, and power plants. Liquid-based cooling methods exploiting the latent heat associated with phase change phenomena, such as nucleate boiling with high volatile liquid, show promise in effectively dissipating high heat fluxes. However, it's important to note that there are challenges related to delayed boiling incipience and temperature excursions that need to be addressed to ensure the longevity and reliability of electronic devices when using this cooling method.

The study of bubble heat transfer mechanisms and their interaction with solid surfaces has been the subject of extensive experimental and numerical investigations. Various models have been proposed to explain bubble heat transfer, including the micro-convection model by Mikic and Rosenhow [1], the microlayer model by Cooper and Lloyd [2], and the contact line model by Stephan and Hammer [3] and Mitrovic [4]. Recent advancements in computer hardware and interface tracking codes have allowed for numerical simulations, such as those conducted by [5-7] to complement experimental studies.

Extensive research has been conducted by numerous authors to understand the boiling characteristics of water. However, the situation is quite different when it comes to high volatile fluids such as FC-72, Novec, HFC-7100, DCM. Surprisingly, there is a noticeable scarcity of literature addressing these volatile substances, with limited attention from dedicated researchers. In the following sections, we will delve into the work of a few authors who have ventured into the realm of high volatile fluids, shedding some light on this relatively unexplored area.

Yaddanapudi and Kim [8] conducted experiments on FC-72 to measure local heat transfer data underneath single bubbles nucleating from a single site. Their results challenged the widely accepted view of microlayer evaporation as the dominant heat transfer mechanism in saturated pool boiling. They found that bubble growth primarily occurred due to energy gained from the superheated liquid layer, and bubble departure resulted in the removal of part of the superheated layer, enabling energy transfer from the wall through transient conduction and/or micro-convection, consistent with the model of Mikic and Rosenhow [1]. Demiray and Kim [9] presented local heat transfer data for bubbles nucleating from a single site from FC-72. They focused on the effect of decreasing the bubble departure diameter, which increases the detaching frequency of the bubbles and enhances nucleate boiling. They used an array with smaller heaters and observed enhancements in nucleate boiling heat transfer coefficient and critical heat flux. Further investigations have been conducted on various surface modifications to enhance nucleate boiling heat transfer. Baldwin et al. [10] studied surfaces with re-entrant cavities and reported higher critical heat flux compared to smooth surfaces. Kubo et al. [11] investigated nucleate boiling of FC-72 on silicon surfaces with re-entrant cavities and observed improvements in the nucleate boiling heat transfer coefficient and critical heat flux. Arbelaez et al. [12] examined saturated boiling on aluminum foam surfaces and found significantly higher nucleate boiling heat flux and critical heat flux compared to a machined aluminum block. El-Genk and Parker [13] reported significant increases in the nucleate boiling heat transfer coefficient and critical heat flux of HFE-7100 on porous graphite surfaces. They observed no temperature excursion at boiling incipience.

Understanding the boiling characteristics of dichloromethane (DCM) is of paramount importance due to its unique properties that set it apart from conventional fluids like water. DCM possesses a remarkably low saturation temperature, making it a very effective coolant for applications involving modern electronic equipment and high-heat-flux scenarios. This exceptional property allows DCM to efficiently absorb and dissipate heat, ensuring the safe operation of electronic components even in compact and high-performance devices where traditional cooling methods may struggle. Despite its potential, the literature lacks comprehensive investigations into DCM's boiling behavior, leaving a substantial knowledge gap regarding its bubble dynamics, heat transfer mechanisms, and overall boiling performance. Given the growing demand for efficient cooling solutions across industries, including electronic equipment and power generation, it becomes imperative to explore the potential of alternative high-volatile fluids like DCM. An in-depth exploration of DCM boiling intricacies promises to yield critical insights that can profoundly influence the design and optimization of advanced cooling systems.

This study aims to fill this critical research gap by conducting a comprehensive examination of DCM boiling characteristics. Through a series of pool boiling experiments under varying heat flux levels, we will investigate key parameters such as bubble departure frequency, bubble diameter, and waiting time, shedding light on the fundamental dynamics of DCM boiling.

2. Materials and Methods

The experimental setup used for the experiments is depicted in Figure 1, showing the pictorial representation of the boiling chamber and the complete setup. The apparatus consists of two main parts: a test cell with optical access chamber and a condenser unit. The test cell has cuboid shape with dimensions of 52 x 82 x 100 mm^3 and is equipped with optical windows on the front and rear walls to allow optical visualization. To control the bulk fluid temperature, 3 k-type thermocouples are installed in the test cell and one of them is connected to a PID controller, which regulates the power supplied to two 300 W cartridge heaters attached to the walls of the test cell. The heating substrate is made of borofloat glass with dimensions of 25 x 25 x 0.7 mm^3 and is coated with indium-tin-oxide (ITO). Two electrodes are connected to the ITO coating using silver epoxy to provide electricity. In the center of the heated substrate, a specific area of the ITO coating is etched away in an I-shape with a size limit of 4 x 5 mm^2. This concentration of thermal energy in the

etched region increases the local resistance to electrical current and leads to the formation of a vapor bubble near the geometric center. DCM is used as the high volatile working fluid and is in direct contact with the top surface of the borofloat borofloat glass. The resistance of the ITO coating is tested between experiments to ensure its stability, and the variation in in resistance remains within 1% of the nominal value of 20. Prior to each experiment, DCM is vigorously boiled to remove remove any dissolved gases. The condenser unit is intermittently turned on and off during the degassing process to rapidly rapidly lower the chamber operating pressure by condensing the generated vapor, promoting effective degassing.

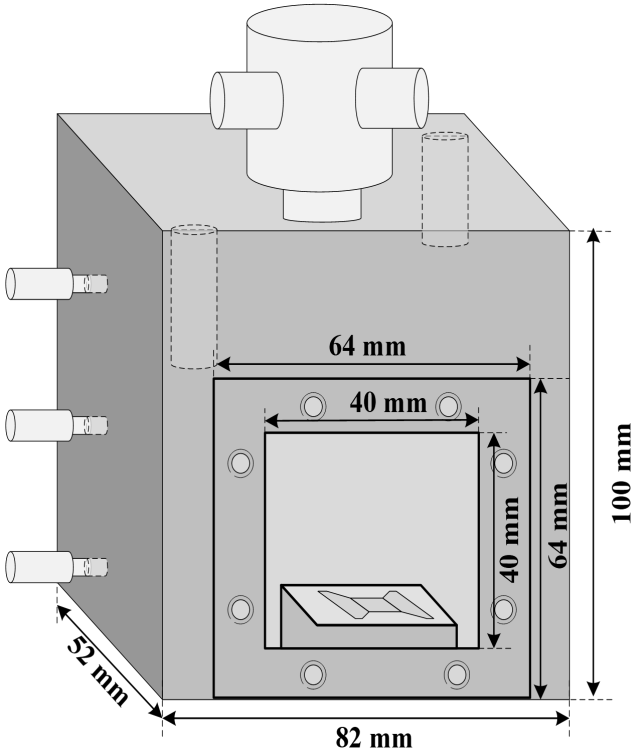

Fig. 1: Schematic diagram of the experimental set-up

The optical setup for imaging the dynamic behavior of the bubble during nucleate boiling is shown in Figure 2, rainbow schlieren deflectometry (RSD) is used for this purpose. To record the growth dynamics of the vapor bubble on the heated substrate surface and map the transients of the microlayer region underneath the bubble, the gradients-based rainbow schlieren deflectometry (RSD) approach is implemented. The RSD method not only maps the bubble dynamics but also provides information about the spatial and temporal distribution of the thermal field in the region of interest.

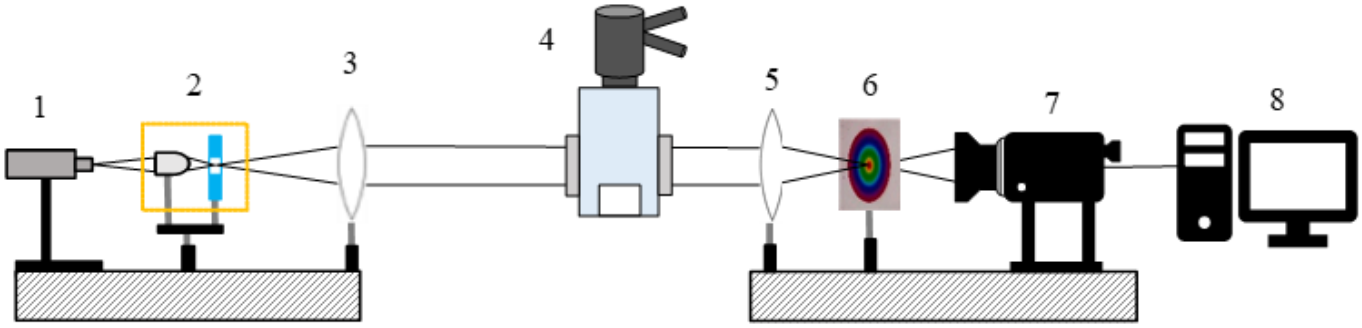

1. White light source 2. Spatial filter arrangement 3. Collimating lens 4. Experimental setup
5. De-collimating lens 6. Rainbow filter 7. High-speed camera 8. Computer

Fig. 2: Schematic illustration of the optical setup for rainbow schlieren deflectometry

Detailed information about the rainbow schlieren setup, including the color filter and the quantitative analysis of captured schlieren images, can be found in previous works by the authors [14]. The schlieren camera recorded boiling phenomena at 5000 fps, with spatial resolution of 35 μm.

The diameter of bubble departure is reported as an equivalent spherical diameter. This is achieved by calculating the diameter of a perfectly spherical bubble that occupies the same volume as the actual vapor bubble. The volume of the vapor bubble is determined using schlieren images, assuming the bubble's axisymmetry and representing it as a stack of circular discs with a thickness equivalent to one pixel. Consequently, the instantaneous volume of the vapor bubble is calculated using the following equations:

$$V = \sum_{i=1}^{i=n} \frac{\pi}{4} D_i^2 \times pixel\ size \tag{1}$$

$$D_{eq} = \sqrt[3]{\frac{6V}{\pi}} \tag{2}$$

In these equations, V represents the instantaneous volume of the vapor bubble, D_i denotes the diameter of the circular disc at the ith position (where i is a pixel index ranging from the base to the apex of the bubble), and D_{eq} corresponds to the instantaneous equivalent diameter of the bubble. MATLAB program is utilized to calculate the bubble's equivalent diameter using the aforementioned equations. The uncertainties associated with the data and the calculated heat flux are listed in Table 1 and the properties of DCM were taken from previous works by the authors [15].

Table 1: Measurement uncertainties for critical experiment parameters.

Parameter	Value	Uncertainty
V (volt)		0.02
I (amp)		0.002
$A_{effective,ITO}$ (m^2)	2×10^{-5}	2×10^{-6}
Temperature (°C)	40°C	1
q (kW/m^2)	58, 76, 95	5, 7,7

3. Result and Discussions

The dynamics of bubbles and temperature gradients in isolated pool boiling of Dichloromethane (DCM) as working fluid under saturated bulk conditions were investigated. The qualitative and quantitative interpretation of the results was based on rainbow schlieren deflectometry, which produced images capturing the growth of a vapor bubble and the wait times for DCM. These images depicted a single vapor bubble generated in a saturated pool of the DCM liquids with different heat flux (58, 76, 95 kW/m^2).

The transients associated with changes in the shape at various stages of the bubble growth process are understood by using the rainbow schlieren deflectometry recorded at saturated bulk conditions with a heat flux of q" = 58 kW/m^2 as shown in figure 3. The research delved into the evolution of the vapor bubble's shape and structure as it incepted, evolved, and traversed various phases throughout its complete growth cycle.

Initially, the vapor bubble displayed a nearly hemispherical shape, maintaining this form until 6.4 ms. Beyond this point, a noteworthy transformation occurred, with the bubble's shape transitioning from hemispherical to nearly spherical as it approached the departure phase.

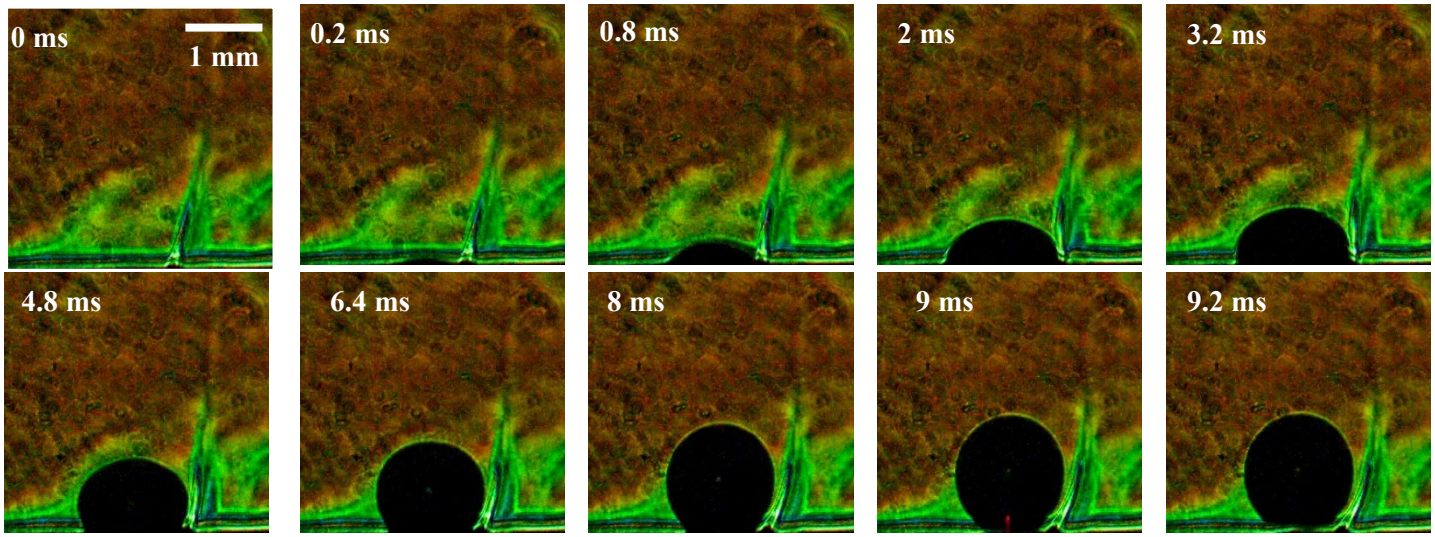

Fig. 3: Time-lapsed photographs of the rainbow schlieren images of single vapor bubble during one complete ebullition cycle

In order to analyze the forces exerted on the bubble throughout its entire growth phase, and gain insights into its growth mechanism, it is essential to examine the bubble growth curve, which illustrates the relationship between its radius and time. The time interval between consecutive frames is 0.2 ms, although the initial reference time (when the bubble radius is zero) in the first image of Figure 3 may lack accuracy. Figure 4 presents the measured bubble radius plotted against time until the bubble's departure in the cycle shown in Figure 3. Evidently, the curve displays a noticeable change in slope after approximately 2 ms, indicating the presence of two growth stages: rapid growth in the period below 2 ms, and slower growth in the period beyond 2 ms. Notably, at the end of the first stage (2 ms), the bubble radius reaches 0.65 mm, which corresponds to approximately 68% of the departure radius (0.95 mm).

The temporal variation of the bubble equivalent radius and its growth rate for various heat fluxes is presented in Figure 4 for the saturated boiling condition of DCM. When the heat flux is increased, the corresponding bubble radius also increases, with a maximum of 0.95 mm being reached when the heat flux value is 95 kW/m^2 and a minimum of 0.6 mm is reached when the heat flux is 58 kW/m^2 at the time of departure. According to the information that has been provided, the process of bubble growth can be categorizedinto three primary regimes: inertia-controlled growth, transition, and diffusion-controlled expansion. In each of these regimes, the relative variances in the slope of the bubble growth curves are different from one another. As an illustration, the initial phase of bubble expansion when subjected to a heat flux of 95 kW/m^2 has a steeper slope in contrast to that of other heat fluxes. When comparing the bubble growth rate at high heat flux with that at low supplied heat flux, it can be seen that the bubble growth rate increases when the heat flux is higher. However, as the bubble grows from an inertia-controlled phase to a diffusion-dominated growth phase, the slope of the curves begins to flatten out before becoming more or less constant. This occurs as the bubble moves from an inertia-controlled phase to a growth phase dominated by diffusion.

The observed relationship between the level of supplied heat flux and the average equivalent bubble departure diameter can also be explained through fundamental principles. The size of the bubble departure diameter is primarily governed by the interplay between two main forces: buoyancy force and surface tension force. The buoyancy force acts in an upward direction, driven by the density difference between the surrounding liquid and the vapor phase inside the bubble. On the other hand, the surface tension force acts in the opposite direction, attempting to minimize the surface area of the bubble. When the level of supplied heat flux decreases, it affects the strength of these forces. A decrease in heat flux leads to a reduction in the intensity of vaporization, which, in turn, results in minimal changes to the density difference between the liquid and vapor phases. As a consequence, the buoyancy force decreases. Simultaneously, the surface tension force also experiences changes. This occurs because the decrease in heat input affects the distribution and behavior of molecules at the liquid-vapor interface, leading to alterations in surface tension forces.

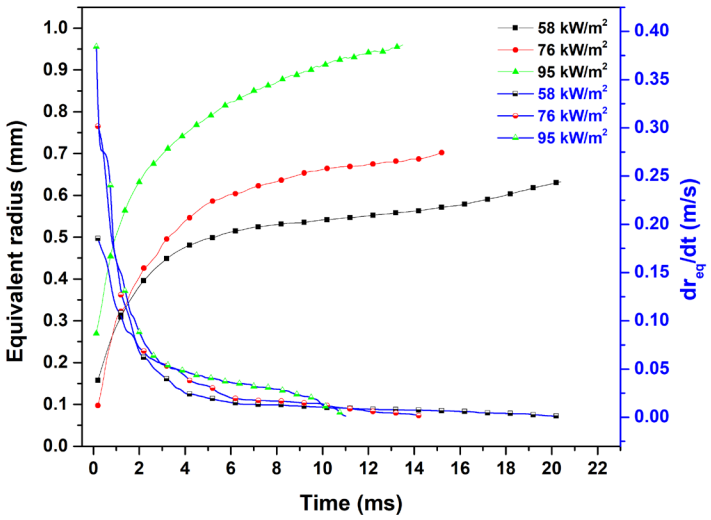

Fig. 4: Equivalent radius and growth rate of DCM bubble as a function of applied heat flux

Bubble dynamic parameters, including bubble departure diameter, departure frequency, growth time, wait time, and volumetric growth rate, were measured using recorded schlieren images for saturated DCM. The growth time represents the duration from the formation of a bubble until its departure, while the wait time is the interval between bubble departure and the subsequent bubble formation as shown in Figure 5 (a). The combined duration of growth time and wait time is known as the ebullition period or cycle. To determine the bubble departure frequency, the ebullition period for each individual bubble was inverted as shown in Figure 5 (b). This provided the rate at which bubbles departed from the heated surface. The departure frequency was calculated for each bubble and subsequently averaged across the total number of bubble cycles.

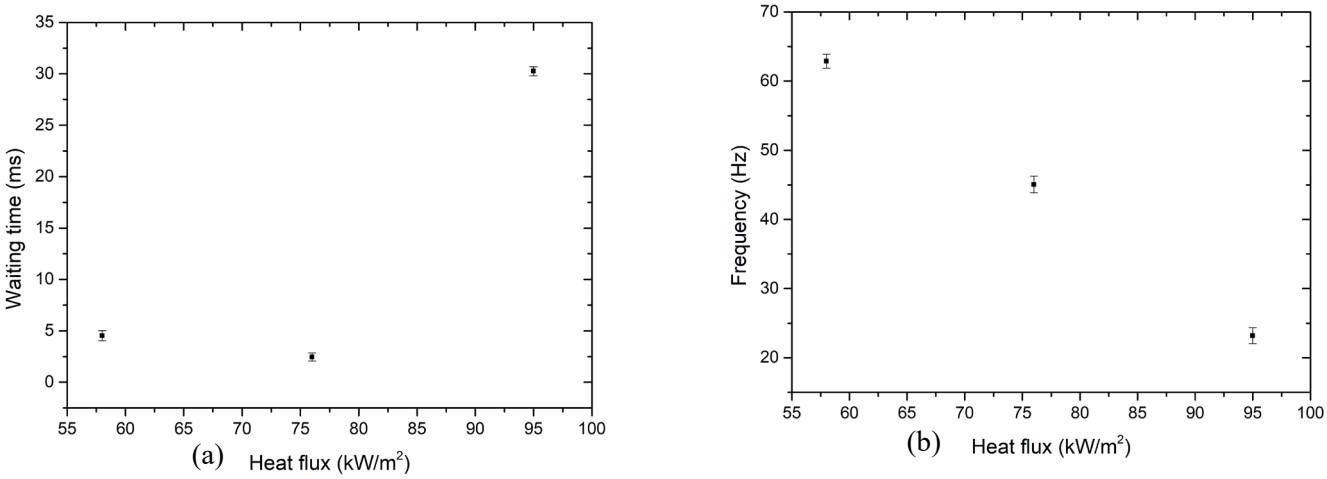

Fig. 5: Relationship between heat flux and (a) waiting time (b) bubble departure frequency

The observed variation in waiting time with increasing heat flux from 4.5 ms to 2.5 ms and then a subsequent increase to 43 ms at the highest heat flux of 95 kW/m^2 can be attributed to the complex interplay of several factors in the bubble nucleation and growth process. The observed changes in waiting time with increasing heat flux are reflection of the intricate and nonlinear nature of bubble formation and growth. However, with the increase in heat flux, the bubble

departure frequency decreases, e.g. the bubble departure frequency was about 63 Hz at 58 kW/m^2 and decreased to about 23 Hz at 95 kW/m^2. The change in waiting time before bubble departure can be understood in terms of bubble dynamics and bubble nucleation. At lower heat flux levels, the waiting time decreases because there is less time required for smaller bubbles to reach the departure size. However, at the highest heat flux value, the waiting time increases again. This can be attributed to the formation of larger bubbles that take longer to reach the departure size, as they require more time to accumulate the necessary vapor mass.

In order to perform a quantitative assessment of the dynamic forces influencing the evolution of the bubble during its growth phase, we adopted a methodology akin to the one detailed by Bucci et al. [16]. The results obtained from this analysis, which encompass various dynamic forces, are illustrated in Figure 6. The computed forces encompass liquid inertia, surface tension, buoyancy, and contact pressure. Notably, the liquid inertia force and surface tension force consistently act in the downward direction, while the contact pressure and buoyancy forces exert an upward influence. Parameters essential for calculating the surface tension and contact pressure forces, including contact radius and contact angle, were directly derived from experimental data. Figure 6 illustrates a notable pattern: during the initial 3 ms, the liquid inertia force predominates over other forces, gradually approaching zero as time progresses. This behavior elucidates the hemispherical bubble morphology depicted in Figure 3 at the onset of bubble growth. In the intermediate stage (3–10 ms), the surface tension force slightly surpasses the buoyancy force, facilitating the gradual transition towards a spherical shape. In the final stage ($\leq$10 ms), a pivotal shift occurs. The combined influence of buoyancy and contact pressure forces overtakes the surface tension force, leading to vertical stretching of the bubble and the formation of a neck, a precursor to departure.

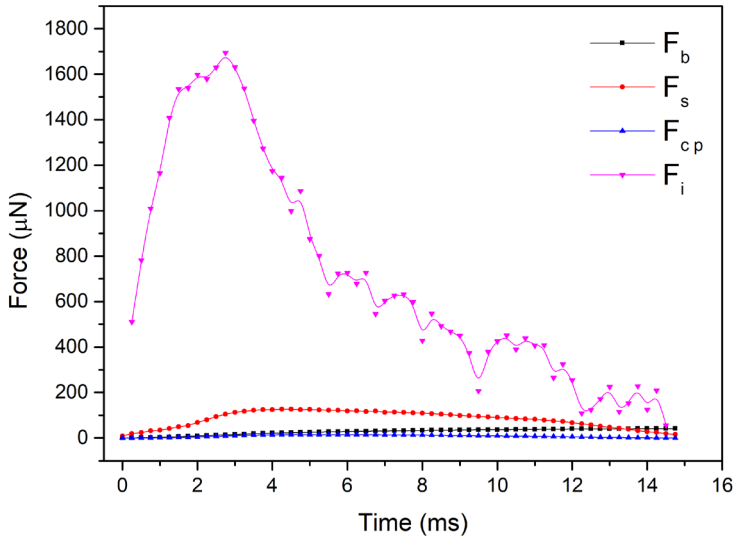

Fig. 6: Various forces acting on the bubble

4. Conclusion

An experimental investigation was conducted to examine the behavior of a highly volatile fluid, dichloromethane (DCM), on a plain surface of indium tin oxide (ITO) coated glass. The focus of the study was to understand the isolated nucleate boiling phenomenon of DCM. Mapping of the dynamics associated with each phenomenon was realized through the application of the gradient-based imaging technique rainbow schlieren deflectometry (RSD). The schlieren images allowed for the measurement of essential bubble characteristics, such as bubble departure diameter, bubble frequency, and waiting time. Through a quantitative analysis of these images, it was discovered that the bubble dynamics underwent significant changes based on the varying levels of heat flux. Three different heat flux levels were investigated: 58, 76, 95 kW/m^2.

The bubble departure diameter exhibited an increase as the heat flux level rose. This implies that higher heat flux led to larger bubble sizes during the boiling process. Furthermore, a comparison of cycle times revealed that the growth time,

referring to the duration of bubble growth from inception to departure, had a dominant influence on the overall cycle for the DCM fluid system. As the heat flux was enhanced, the overall cycle time increased considerably. Consequently, this prolonged cycle time caused a decrease in the bubble departure frequency, indicating a reduced rate at which bubbles departing from the heated surface. The various forces affecting bubble growth were calculated. Initially, the dominant is liquid inertia, causing a hemispherical shape. As time progresses, surface tension surpasses buoyancy, leading to a more spherical shape. In the final stage, buoyancy and contact pressure forces prevail, resulting in vertical stretching and the formation of a neck before bubble departure. Towards the end of this section, importance of the work reported needs to be highlighted. In what way it has contributed to the existing physics.

References

[1] B.B. Mikic and W.M. Rosenhow, "Bubble growth rates in nonuniform temperature field," *Prog. Heat Mass Transfer II* (1969) 283–292.

[2] M.G. Cooper and A.J.P. Lloyd, "The microlayer in nucleate boiling," *Int. J. Heat Mass Transfer* 12 (1969) 895–913.

[3] P. Stephan, and J. Hammer, "A new model for nucleate boiling heat transfer", *Heat and Mass Transfer*, 30(2) (1995) pp.119-125.

[4] J. Mitrovic, "Flow and heat transfer in the wedge-shaped liquid film formed during the growth of a vapour bubble," *Int. J. Heat Mass Transfer* 41 (12) (1998) 1771–1785.

[5] S.W. Welch, "Direct simulation of vapor bubble growth," *Int. J. Heat Mass Transfer* 41 (1998) 1655–1666.

[6] G. Son, V.K. Dhir, N. Ramanujapu, "Dynamics and heat transfer associated with a single bubble during nucleate boiling on a horizontal surface," *J. Heat Transfer* 121 (1999) 623–631.

[7] Yoon, Koshizuka, Oka, "Direct calculation of bubble growth, departure and rise in nucleate boiling," *Int. J. Multiphase Flow* 27 (2001) 277–298.

[8] N. Yaddanapudi and J. Kim, "Single bubble heat transfer in saturated pool boiling of FC-72," *Multiphase Sci. Technol.* 12 (3–4) (2001) 47–63.

[9] Demiray and Kim, "Heat transfer from a single nucleation site during saturated pool boiling of FC-72 using an array of 100 micron heaters," *in: Proceedings of the 2002 AIAA/ ASME Joint Thermophysics Conference, St. Louis, MO*, 2002.

[10] C. Baldwin, S. Bhavnani, R. Jaeger, "Towards optimizing enhanced surfaces for passive immersion cooled heat sinks," *in: Proc. Intersociety Conf. on Thermal and Thermotechnical Phenomena in Electronic Systems*, 1998, pp. 399– 407.

[11] H. Kubo, H. Takamatsu, H. Honda, "Effects of size and number density of micro-reentrant cavities on boiling heat transfer from a silicon chip immersed in degassed and gas dissolved FC-72," *J. Enhanced Heat Transfer* 6 (2–4) (1999) 151–160.

[12] F. Arbelaez, S. Sett, R. Mahajan, "An experimental study on pool boiling of saturated FC-72 in highly porous aluminum foams," *in: Proc. of 34th National Heat Transfer Conf.*, vol. 1, 2000, pp. 759–767.

[13] M. El-Genk and J. Parker, "Enhanced boiling of HFE-7100 dielectric liquid on porous graphite," *Energy Conversion Manage*. 46 (2005) 2455–2481.

[14] Kumar, A., Kangude, P. and Srivastava, A., "Coupled bubble dynamics and interaction mechanisms of adjacently nucleated vapor bubbles under subcooled pool boiling regime." *Phys. Fluids* 35, no. 8 (2023).

[15] A. Kumar, C. Hinduja, and A. Srivastava, "Non-intrusive diagnostics of differentially-heated two-component immiscible fluid layer with phase change," *International Communications in Heat and Mass Transfer* 140 (2023): 106513.

[16] M. Bucci, J. Buongiorno, M. Bucci, "The not-so-subtle flaws of the force balance approach to predict the departure of bubbles in boiling heat transfer," *Phys. Fluids* 33 (1) (2021) 017110 .